URSI GASS 2020, Rome, Italy, 29 August - 5 September 2020

Sea ice detection using Ku-band radar onboard GPM satellite

M. Panfilova(1), A. Shikov(2), and V. Karaev(1)
(1) Institute of applied physics RAS, Nizhny Novgorod, Russia
(2) Lobachevsky state university, Nizhny Novgorod, Russia

Abstract

The method for automatic sea ice detection by DPR data is suggested. The method is based on the analysis of the shape of normalized radar cross section dependence on the incidence angle. For refinement of ice position along the track one dimensional Canny edge detection procedure is applied. The data for winter 2016 were processed for the Sea of Okhotsk. The algorithm was validated using the radiometer data.

1 Introduction

Sea ice cover monitoring from space is an important problem for navigation, weather prediction and climate analysis. Microwave spaceborne measurements are widely used to create ice cover maps. For determining the ice concentration microwave radiometer and synthetic aperture radar data is used. Altimeter data is applied to detect ice thickness. However, manifestations of sea ice in microwave signal are not studied for incidence angles between 0° and 18°. At such angles dual-frequency precipitation radar (DPR) on Global precipitation measurement (GPM) satellite operates, as well as SWIM (Surface Waves Investigation and Monitoring instrument) which is of great interest now. This paper is focused on the DPR radar, Ku-band channel, which scanning direction is perpendicular to the track. There are no ice flags for DPR derived from its own data by now. This paper suggests the simple method for automatic sea ice detection from Ku-band the data of normalized radar cross section (NRCS).

2 Data

The GPM satellite was launched in February 2014, carrying five instruments including the DPR and radiometer GPM Microwave Imager (GMI). The satellite ground track is confined between 65° S and 65° N. The DPR is a Ku- and Ka-band pulsed radar with horizontal polarization, further we consider Ku-band radar only because it had a wider ground track in 2016. The DPR antenna scans perpendicularly to the flight direction. The scanning angle varies from -17° to +17°, with 49 beam positions separated by 0.71°. The local incidence angle depends on the shape of the Earth. Maximum local incidence angle is approximately 18°, spatial resolution is about 5 km by 5 km. The GPM data contains a rain flag for each resolution element. The DPR swath in Ku-band over the Sea of Okhotsk, December 27th, 2016 is mapped in figure 1a, and typical dependence of NRCS on incidence angle along the scanning direction for water and ice surfaces are presented in the figure 1b. Clear difference between them is observed. The idea is to obtain the scalar value from each scan $\sigma^0(\theta)$ and distinguish between "ice" and "water" scans.

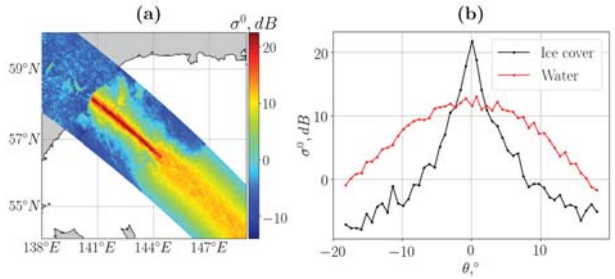

Figure 1. The DPR Ku-band swath over the Sea of Okhotsk, December 27th, 2016 (a), the sections of the swath in the region of ice and water (b)

3 Ice detection method

3.1 Backscatter at low incidence angles

Backscatter of microwaves by the sea surface at low incidence angles is conveniently described within the framework of geometrical optics approximation. According to this approximation NRCS is proportional to the slope probability density function (PDF) along the direction of scanning [2]

$$\sigma^0 = A\cos^{-4}(\theta)\cdot P(\tan\theta) \qquad (1)$$

It was shown in [4], that this PDF for sea surface is close to normal distribution.

$$P(\tan\theta) = \frac{1}{2\pi\sigma_x\sigma_y}\cdot\exp(-\frac{\tan^2\theta}{2\sigma_x^2}) \qquad (2)$$

where $\sigma^2_{x,y}$ are mean square slopes along and across scanning direction respectively. This approximation is valid for incidence angles within the range $0° < \theta < 15°$ according to [1].

3.2 Analysis of the data along the scan

The peculiarity of the sea ice the slope PDF is the narrow peak at $\theta = 0^\circ$. The presence of this peak can be explained by the fact that for almost flat ice cover there are much less facets tilted from the horizontal than for water surface. PDF for water has a wide peak. It is known that the kurtosis describes the sharpness of a peak of the curve of probability density and the steepness of slopes of the distribution tails. The sharper is the curve peak near the center of distribution, the greater is the value of the kurtosis. The kurtosis for $P(x)$ PDF is calculated as follows

$$\gamma_2 = \frac{\mu_4}{\mu_2^2} - 3, \tag{3}$$

where μ_2 and μ_4 are the central statistical moments of PDF

$$\mu_k = \int_{-\infty}^{\infty} (x - \bar{x})^k P(x) dx \tag{4}$$

and $\bar{x}$ is the expected value of x:

$$\bar{x} = \int_{-\infty}^{\infty} x P(x) dx. \tag{5}$$

From (1) the slope PDF $P(\tan\theta)$ is easily retrieved for each i^{th} antenna footprint

$$P(\tan\theta_i) = \frac{\sigma_i^0 \cos^4(\theta_i)}{A}. \tag{6}$$

Due to the fact that cumulative distribution function $F(X)$ at $+\infty$ equals to 1

$$F(+\infty) = \int_{-\infty}^{\infty} P(\tan\theta) d(\tan\theta) = 1. \tag{7}$$

At incidence angles higher than 15° $P(\tan\theta)$ takes low values and the integral for this angles can be neglected. This condition in a discrete form is as follows

$$\int_{\tan(-15^\circ)}^{\tan(+15^\circ)} P(\tan\theta) d(\tan\theta) \approx \sum_{i=1}^{N} P(\tan\theta_i) \Delta(\tan\theta_i) = 1. \tag{8}$$

If we consider the part of the scan for $-15^\circ\theta 15^\circ$, $N = 41$. From this equation the coefficient A is obtained

$$A = \sum_{i=1}^{N} \sigma_i^0 \cos^4(\theta_i) \Delta(\tan\theta_i). \tag{9}$$

For each i $\Delta(\tan\theta_i) = \Delta\theta_i \cos^{-2}(\theta_i)$ is almost constant, thus from (6) and (9) the equation for μ_k in a discrete form is as follows

$$\mu_k = \sum_{i=1}^{N} (\tan\theta_i - \overline{\tan\theta_i})^k P(\tan\theta_i) \Delta(\tan\theta_i) =$$

$$= \sum_{i=1}^{N} (\tan\theta_i - \overline{\tan\theta_i})^k \sigma_i^0 \cos^4(\theta_i) \left[\sum_{i=1}^{N} \sigma_i^0 \cos^4(\theta_i) \right]^{-1}. \tag{10}$$

Each half of the swath can be considered separately for $\theta > 0^\circ$ and $\theta < 0^\circ$. In order to calculate kurtosis properly each half is complemented symmetrically so that $\sigma^0(\theta) = \sigma^0(-\theta)$ and for each augmented half-scan the operations (3)-(10) are performed. In figure 3 the radar swath and corresponding kurtosis, calculated for each complemented half-scan, are presented. It is clearly seen that

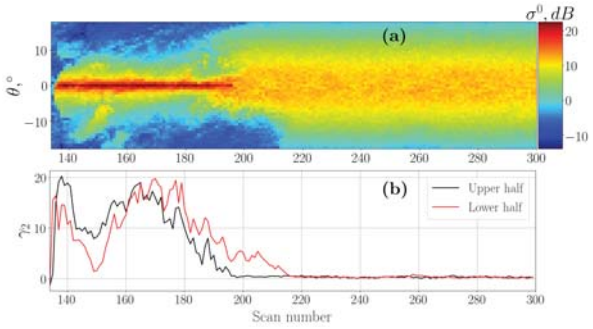

Figure 2. The NRCS distribution within DPR swath (a), kurtosis calculated for each complemented half-scan (b).

for water $\gamma_2 \approx 0$ and for ice it reaches 20.

In the next section the rectification of water-ice boundary along the track is discussed.

3.3 Analysis of the data along the flight direction

This section is devoted to the edge detection problem from the radar image of DPR. The two-dimensional edge detection can not be directly applied because of the NRCS trend associated with incidence angles. Therefore the one-dimensional Canny edge detection algorithm [3] was adapted to solve the problem.

Now let us consider the slice of the swath along the scanning direction at a constant incidence angle. The lengthwise slices for several incidence angles are presented in figure 3a. At nadir the difference $\sigma^0_{ice} - \sigma^0_{water}$ is positive, at $6^\circ - 18^\circ$ the reverse situation is observed. At intermediate angles about $2^\circ - 5^\circ$ there is almost no contrast between the two surfaces.

According to [3] the position of the step corresponds to the maximum of the following function

$$Q(x_0) = \frac{\left| \int_{-W}^{+W} \sigma^0(x_0 - x) f(x) dx \right|}{n_0^2 \sqrt{\int_{-W}^{+W} f^2(x) dx}} \frac{\left| \int_{-W}^{+W} \sigma^{0\prime}(x_0 - x) f'(x) dx \right|}{\sqrt{\int_{-W}^{+W} f'^2(x) dx}}, \tag{11}$$

where x is the coordinate along the flight direction, the prime means the derivative by x, n_0 is the noise level which we consider to be constant, $f(x)$ is proportional to the first derivative of gaussian function

$$f(x) = -x \cdot \exp(-\frac{x^2}{2\sigma_g^2}). \tag{12}$$

Actually, the whole denominator is constant and we search the maximum of

$$S(x_0) = \left| \int_{-W}^{+W} \sigma^0(x_0 - x) f(x) dx \right| \left| \int_{-W}^{+W} \sigma^{0\prime}(x_0 - x) f'(x) dx \right|, \quad (13)$$

Here W and σ_g are the parameters to be adjusted. In figure 3b the function $S(x_0)$ is plotted for $\theta = 14^\circ$ with $W = 20$ cells and $\sigma_g = 5$ cells. Local maxima of $S(x_0)$

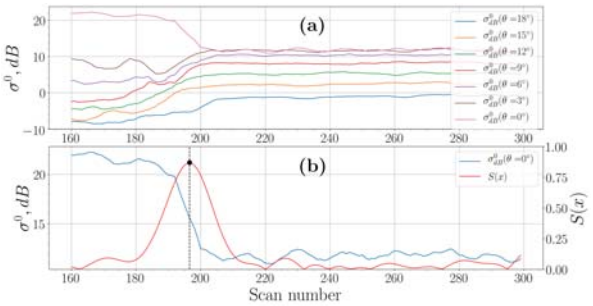

Figure 3. The NRCS along the swath at water-ice boundary for several incidence angles (a), function $S(x_0)$ calculated by the equation (13) for incidence angle $\theta = 14^\circ$

were obtained, and in order to pick the pixels, corresponding to the ice edge, double thresholding was used. The low threshold is $S_L = 0.15(S_{max} - S_{min})$ and the high threshold is $S_H = 0.7(S_{max} - S_{min})$. The local maxima pixels with $S \geq S_H$ are denoted as strong edges; with $S < S_L$ are neglected and $S_L \leq S < S_H$ are denoted as weak edges. Strong edges are automatically marked in the final edge image, and weak edges are included if they are connected to strong edges.

4 Results and discussion

The algorithm was applied to the radar swath mapped in figure 1a. For validation the ice cover map created by SRC "Planeta" was used. The high values of kurtosis from DPR data are observed over the ice cover, marked as a shaded area in figure 4a.

Each map contains an average position of ice cover over the span of three days, therefore for validation of ice edge detection the radiometer data was used.

In figure 4b the brightness temperature measured by GMI radiometer is mapped for 36.6 GHz, horizontal polarization, at the same moment as DPR microwave image was taken. The boundary position defined from the radar data corresponds to the contrast in T_b.

Good agreement with the ice cover maps and radiometer data proves the validity of the algorithm. Further markup of the swath, assignment the ice or water status to the cells in the radar swath, requires the analysis of a large set of swaths in order to adjust threshold values for kurtosis and other parameters.

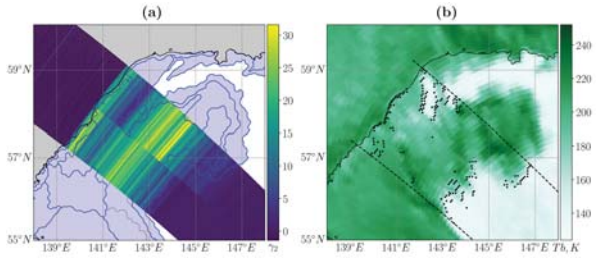

Figure 4. The values of kurtosis for DRP complemented half-scans over the sea ice map (a); brightness temperature measure by GMI radiometer (color) and the NRCS steps from the DPR data (dots) (b).

5 Conclusion

The method for automatic ice detection from DPR data is developed. On the first step the kurtosis of the slope PDF is estimated from $\sigma^0(\theta)$ for each scan, which can help to obtain the express estimate of ice position from the DPR data. On the second step the lengthwise slices of the swath for each incidence angle are studied to obtain the step in NRCS, corresponding to the water-ice boundary. Good agreement with radiometer and ice cover maps is obtained. Basing on the results of these two estimates further markup of the swath can be performed.

6 Acknowledgements

This work was supported by Russian Science Foundation (Project RSF 20-17-00179).

References

[1] M. H. Freilich, "The relationship between winds, surface roughness, and radar backscatter at low incidence angles from TRMM precipitation radar measurements," *Space Weather*, **11**, 4, April 2003, pp. 138–139, doi:10.1175/1520-0426(2003)20<549:TRBWSR>2.0.CO;2.

[2] F. G. Bass and I. M. Fuks, "Scattering of waves by statistically rough surfaces," Pergamon Press, 1972.

[3] J. Canny, "Scattering of waves by statistically rough surfaces," *IEEE Transactions on Pattern Analysis and Machine Intelligence*, **PAMI-8**, 6, November 1986, pp. 679–698, doi: 10.1109/TPAMI.1986.4767851.

[4] X. Chu and Y. He and G. Chen, "Asymmetry and Anisotropy of Microwave Backscatter at Low Incidence Angles," *IEEE Transactions on Geoscience and Remote Sensing*, **50**, 10, October 2012, pp. 4014–4024, doi: 10.1109/TGRS.2012.2189010.